EUROPEAN ORGANIZATION FOR NUCLEAR RESEARCH

CERN-EP/2000-107
August 23, 2000

Measurement of Bose-Einstein Correlations in $e^+e^- \rightarrow W^+W^-$ at $\sqrt{s} \simeq 189$ GeV

The L3 Collaboration

Abstract

We investigate Bose-Einstein correlations (BEC) in W-pair production at $\sqrt{s} \simeq$ 189 GeV using the L3 detector at LEP. We observe BEC between particles from a single W decay in good agreement with those from a light-quark Z decay sample. We investigate their possible existence between particles coming from different W's. No evidence for such inter-W BEC is found.

Submitted to *Phys. Lett. B*

Introduction

Bose-Einstein (BE) interference is observed as an enhanced production of identical bosons, *e.g.*, charged pions, at small four-momentum difference in elementary particle and nuclear collisions [1, 2], and, in particular, in hadronic Z decay [3, 4]. Such an interference should also be present in hadronic W decay (intra-W BE interference). Furthermore, since in fully hadronic WW events ($\mathrm{e^+e^-} \to \mathrm{W^+W^-} \to \mathrm{q\overline{q}q\overline{q}}$), the W decay products overlap in space-time, interference between identical bosons originating from different W's can be expected [5–7]. This inter-W BE interference may provide a laboratory to measure the space-time development of this overlap. Moreover, this effect, like colour reconnection [6, 8–12], can be a source of bias in the determination of the W mass in the four jet channel. Recent model predictions [5–7], as well as recent experimental results [13], are still contradictory.

The main question we address in this paper is, therefore, whether inter-W BE interference exists. However, we also examine all BE interference, intra-W as well as inter-W, and make a comparison with that observed in hadronic Z decays, with and without the contribution of $\mathrm{Z} \to \mathrm{b\bar{b}}$ decays.

Analysis Method

Bose-Einstein interference manifests itself through correlations between identical bosons at small four-momentum difference. Correlations between two particles are described by the ratio of the two particle number density, $\rho_2(p_1, p_2)$, to the product of the two single particle number densities, $\rho_1(p_1)\rho_1(p_2)$. Since we are only interested in Bose-Einstein correlations (BEC) here, the product of single particle densities is replaced by $\rho_0(p_1, p_2)$, the two particle density that would occur in the absence of Bose-Einstein interference, resulting in the BE correlation function

$$R_2(p_1, p_2) = \frac{\rho_2(p_1, p_2)}{\rho_0(p_1, p_2)} \quad . \tag{1}$$

For identical bosons, $R_2 - 1$ is related to the space-time particle density through a Fourier transformation [2, 14].

Since we shall consider only pion pairs, the mass of the particles is fixed and the correlation function is defined in six-dimensional momentum space. Since Bose-Einstein correlations are largest at small four-momentum difference, $Q \equiv \sqrt{-(p_1 - p_2)^2}$, we parametrize R_2 in terms of this single variable. While this is an oversimplification, as recent two- and three-dimensional analyses have shown [4], lack of statistics prevents such multi-dimensional analyses here.

The following method [15] is used to study inter-W BEC. If the two W's decay independently, the two particle density in fully hadronic WW events, ρ_2^{WW}, is given by

$$\rho_2^{\mathrm{WW}}(p_1, p_2) = \rho_2^{\mathrm{W^+}}(p_1, p_2) + \rho_2^{\mathrm{W^-}}(p_1, p_2) + \rho_1^{\mathrm{W^+}}(p_1)\,\rho_1^{\mathrm{W^-}}(p_2) + \rho_1^{\mathrm{W^-}}(p_1)\,\rho_1^{\mathrm{W^+}}(p_2) \quad , \tag{2}$$

where the superscript, $\mathrm{W^+}$ or $\mathrm{W^-}$, indicates the W which produced the particles. Assuming that the densities for $\mathrm{W^+}$ and $\mathrm{W^-}$ are the same, eq. (2) becomes

$$\rho_2^{\mathrm{WW}}(p_1, p_2) = 2\rho_2^{\mathrm{W}}(p_1, p_2) + 2\rho_1^{\mathrm{W}}(p_1)\,\rho_1^{\mathrm{W}}(p_2) \quad . \tag{3}$$

The terms ρ_2^{WW} and ρ_2^{W} of eq. (3) are measured in the fully hadronic WW and the semi-hadronic events, respectively. To measure the product of the single particle densities, we use the two particle density $\rho_{\mathrm{mix}}^{\mathrm{WW}}(p_1, p_2)$ obtained by pairing particles originating from two different semi-hadronic WW events ($W^+W^- \to \ell\nu q\overline{q}$), since by construction these pairs of particles are uncorrelated.

The hypothesis that the two W's decay independently can be tested using eq. (3). In particular, we write eq. (3) in terms of Q and use the test statistics

$$\Delta\rho(Q) = \rho_2^{\mathrm{WW}}(Q) - 2\rho_2^{\mathrm{W}}(Q) - 2\rho_{\mathrm{mix}}^{\mathrm{WW}}(Q) \tag{4}$$

and

$$D(Q) = \frac{\rho_2^{\mathrm{WW}}(Q)}{2\rho_2^{\mathrm{W}}(Q) + 2\rho_{\mathrm{mix}}^{\mathrm{WW}}(Q)} \quad . \tag{5}$$

The advantage of this method is that it gives access to the inter-W correlations directly from the experimental data; there is no need for normalisation by a Monte Carlo (MC) model.

It is possible that the event mixing procedure introduces artificial distortions and that it does not fully account for some non-BE correlations or some detector effects. To diminish the effect of such inadequacies and to be able to compare more directly to other experiments, we also use the double ratio

$$D'(Q) = \frac{D(Q)}{D_{\mathrm{MC,\,noBE}}(Q)} \quad , \tag{6}$$

where $D_{\mathrm{MC,\,noBE}}$ is derived from a Monte Carlo sample with no BEC, or at least without inter-W BEC.

In the absence of inter-W correlations, $\Delta\rho = 0$ and $D = D' = 1$. To study BEC, we examine these relations for small values of Q, for like-sign particles. To judge the influence of other correlations on these quantities, we examine them also for unlike-sign particles and in Monte Carlo models.

Data Selection

The data used in this analysis were collected in 1998 by the L3 detector [16], and correspond to an integrated luminosity of about 177 pb^{-1} at a centre-of-mass energy of $\sqrt{s} \simeq 189$ GeV.

To obtain the two W^+W^- event samples, one fully hadronic and the other semi-hadronic, we reconstruct the visible final state fermions, *i.e.*, electrons, muons, τ jets (corresponding to the visible τ-decay products) and the hadronic jets corresponding to quarks, and apply the selection criteria described in Ref. [17], with the additional requirement for the fully hadronic channel that the neural network output must be greater than 0.6. In total, 1032 semi-hadronic events and 1431 fully hadronic events are selected.

The event generator KORALW [18] is used to simulate the signal processes. Within KORALW BEC are simulated using the so-called BE_{32} or BE_0 algorithms *) [7]. For most comparisons we will use BE_{32}, since in these comparisons we find it to agree better with the data. Further, the Q distribution of unlike-sign particles is less distorted by BE_{32}. Where BE_0 is used it will be explicitly stated. The BEC are implemented for *all* particles, which we refer to as BEA, or only for particles coming from the *same* W (intra-W BEC), which we refer to as BES. The background processes $e^+e^- \to Z/\gamma \to q\overline{q}$, $e^+e^- \to ZZ$ and $e^+e^- \to Ze^+e^-$ (the last relevant only to the $q\overline{q}e\nu$ and $q\overline{q}\tau\nu$ channels) are generated using PYTHIA [19] with BE_0. The generated events are passed through the L3 detector simulation program [20], reconstructed and subjected to the same WW selection criteria as the data.

*) The BE_{32} algorithm used the parameter values PARJ(92)=1.68 and PARJ(93)=0.38 GeV, whereas BE_0 used PARJ(92)=1.50 and PARJ(93)=0.33 GeV. Both have been tuned to the L3 Z decay data.

MC studies using the above generators show that the selection efficiency for fully hadronic events changes by less than 0.5% when BEC (intra-W, or both intra-W and inter-W) are included. The efficiencies for the channels $\mathrm{q\bar{q}}\ell\nu$, ($\ell = \mathrm{e}, \mu, \tau$) and $\mathrm{q\bar{q}q\bar{q}}$ are found to be 82.9%, 76.7%, 50.6% and 87.2%, respectively. The fractions of background for these channels are 4.1%, 4.1%, 12.7% and 18.6%, respectively.

The BEC study is based on charged particle information from the central tracker. Charged tracks are required to have at least 35 (of 62 possible) hits, and the number of wires from the first to the last hit is required to be at least 45. The distance of closest approach (projected onto the transverse plane) of a track to the nominal interaction vertex is required to be less than 7.5 mm. The transverse momentum of a track must be greater than 100 MeV. After the track selection, there are 287k pairs of like-sign particles in the fully hadronic channel and 55k pairs in the semi-hadronic channel.

With this selection, reasonable agreement is obtained between the data and the MC simulation for the distributions of Q and the difference in azimuthal, as well as polar, angle with respect to the beam, for pairs of like-sign tracks, in both the fully hadronic and the semi-hadronic channels. This is shown in Fig. 1, where the raw data are compared to simulated KORALW with BES and background events. Similar agreement is observed when BEA is used.

Measurement of R_2

We first measure the BE correlation function, R_2, for like-sign charged pion pairs using two choices of reference sample, *i.e.*, the sample from which ρ_0 is determined. The first choice uses a Monte Carlo model without BEC:

$$\rho_0(\pm,\pm) = \rho_2(\pm,\pm)_{\mathrm{MC,\,noBE}} \quad . \tag{7}$$

The second choice uses unlike-sign particle pairs from the experimental events. A major drawback of this method is that the correlation function is affected by the presence of dynamical correlations, such as the decay of resonances. To compensate for this, the density for unlike-sign pairs is multiplied by the ratio of the densities for like- and unlike-sign pairs determined from a Monte Carlo model without BEC:

$$\rho_0(\pm,\pm) = \rho_2(+,-) \cdot \left[\frac{\rho_2(\pm,\pm)}{\rho_2(+,-)}\right]_{\mathrm{MC,\,noBE}} \quad . \tag{8}$$

In both cases we need to correct the correlation function, R_2, for detector resolution, acceptance, efficiency and for particle misidentification. For this we use a multiplicative factor derived from Monte Carlo studies. Since we do not perform explicit hadron identification, this factor is given by the ratio of $\rho_2(\pm,\pm)$ and $\rho_2(\pm,\pm)/\rho_2(+,-)$, respectively, found from Monte Carlo, for *pions* at generator level to that found using *all particles* after full detector simulation, reconstruction and selection. Thus, using eqs. (7) and (8) leads, respectively, to

$$R_2 = \left[\frac{\rho_2(\pm,\pm)_{\mathrm{data}}}{\rho_2(\pm,\pm)_{\mathrm{MC,\,noBE}}}\right] \cdot \left[\frac{\rho_2(\pm,\pm)_{\mathrm{gen}}}{\rho_2(\pm,\pm)_{\mathrm{det}}}\right]_{\mathrm{MC}} \tag{9}$$

and

$$R_2 = \left[\frac{\rho_2(\pm,\pm)}{\rho_2(+,-)}\right]_{\mathrm{data}} \cdot \left[\frac{\rho_2(+,-)}{\rho_2(\pm,\pm)}\right]_{\mathrm{MC,\,noBE}} \cdot \left[\frac{\rho_2(\pm,\pm)_{\mathrm{gen}}}{\rho_2(\pm,\pm)_{\mathrm{det}}} \cdot \frac{\rho_2(+,-)_{\mathrm{det}}}{\rho_2(+,-)_{\mathrm{gen}}}\right]_{\mathrm{MC}} \quad . \tag{10}$$

Background is taken into account by replacing $\rho_{2\,\mathrm{data}}$ in the above equations by

$$\rho_{2\,\mathrm{data-bg}} = \frac{1}{\mathcal{P} N_{\mathrm{ev}}} \left(\frac{\mathrm{d}n}{\mathrm{d}Q} - \frac{\mathrm{d}n_{\mathrm{bg}}}{\mathrm{d}Q} \right) \quad , \tag{11}$$

where $\mathcal{P}$ is the purity of the selection, n is the number of pairs of tracks in the N_{ev} data events, and n_{bg} is the number of pairs of tracks corresponding to $(1-\mathcal{P})N_{\mathrm{ev}}$ background events. The background is estimated using Monte Carlo. In determining R_2 using eq. (9), we use KORALW without BEC as the reference sample. For the detector correction, BES with the BE_{32} algorithm is used for both eqs. (9) and (10).

Fig. 2 shows the correlation function, eq. (9), for the fully hadronic and for the semi-hadronic WW events. We parametrize the Bose-Einstein enhancement at low Q values by

$$R_2(Q) = \gamma(1+\delta Q)(1+\lambda \exp(-R^2 Q^2)) \quad , \tag{12}$$

where γ is an overall normalization factor, the term $(1+\delta Q)$ takes into account possible long-range momentum correlations, λ measures the strength of the BE correlations and R is related to the source size in space-time. The results of the fits of eq. (12) are also shown in Fig. 2.

The fit results for both choices of reference sample, eqs. (7) and (8), are given in Table 1. The statistical error includes the effect of bin-to-bin correlations. Rather than to estimate the full covariance matrix for the bins of the $R_2(Q)$ distribution, we have performed the fit using only the diagonal elements and corrected for this neglect of correlations using Monte Carlo. Using PYTHIA, we generated 100 sets of $\mathrm{W}^+\mathrm{W}^-$ BES events, each with the same statistics as the data. For each set the R_2 distribution was found. Then for each bin in Q the ratio, $S_{\mathrm{bin-bin}}$, of the Gaussian width of R_2 to the average estimated error on R_2 was computed. $S_{\mathrm{bin-bin}}$ was found to be independent of Q. This indicates that a fit ignoring bin-to-bin correlations will yield the correct values of the parameters, but that its χ^2 needs to be multiplied by $1/S^2_{\mathrm{bin-bin}}$ and the errors on the parameters by $S_{\mathrm{bin-bin}}$. As a further check, the R_2 distribution of each set of MC events was fitted, and the variation of γ, λ, R and δ from their average values was determined. The ratio of the Gaussian width to the average fit error was found, providing an alternative determination of $S_{\mathrm{bin-bin}}$ for each parameter. Within statistical errors, this ratio was the same for each parameter and the same as that determined from the $R_2(Q)$ distribution.

The systematic uncertainty is computed by varying the track and event selections. Both stronger and weaker cuts are applied to the tracks, slightly different event selections are made, and the background fractions are varied. The influence of the choice of the Monte Carlo used for the reference sample and for the correction factor is also taken into account. Part of the systematic uncertainty comes from the choice of the fit range. The large systematic uncertainty on λ in the fully hadronic channel is mainly due to the difference of including or not including inter-W BEC in the MC for the correction factor. Using inter-W BEC in the correction factor increases the measured value of λ. The contributions to the systematic uncertainty of λ are shown in Table 2.

BEC are observed ($\lambda > 0$) in both fully hadronic and semi-hadronic WW events. The values of λ are higher for the semi-hadronic than for the fully hadronic channel, but the difference, for each choice of reference sample, is only about two standard deviations using only the statistical error and 1.7 standard deviations using in addition the systematic uncertainty from inter-W BEC on the correction factor. If true, this difference in λ would indicate a suppression of inter-W BEC [15], which we study in detail in the following section.

Since, apart from the quark flavour, hadronic W and Z decays are expected to be similar, we also analyse a high statistics hadronic Z decay sample, collected by the L3 detector in 1994 at

$\sqrt{s} \simeq 91.2$ GeV. Since b quarks are greatly suppressed in W decays, a b-tagging procedure [21] is used to reduce the $b\bar{b}$ fraction in Z decays, from 22% to 3%. The BE correlation function, eq. (9), of the resulting 180k Z events is plotted in Fig. 2b as a full histogram. As expected, good agreement is observed between this histogram and the correlation function of the semi-hadronic WW events. When b quark decays of the Z are not removed from the sample, a depletion of the correlation function at small Q is observed and a clear discrepancy exists with the W data, as the dashed histogram in Fig. 2b shows.

Measurement of Inter-W Bose-Einstein Correlations

The Event Mixing Procedure

To compute the test statistics, eqs. (4) and (5), we need to construct the two particle density $\rho_{\text{mix}}^{\text{WW}}$. This is done by combining pairs of semi-hadronic events having oppositely charged hadronically decaying W's. Particles identified as decay products of the leptonically decaying W's are discarded. Then the particles from one of the events are rotated so that the W's are approximately back-to-back. Since real fully hadronic WW events have a small longitudinal energy imbalance that we ascribe to initial state radiation and since experimental resolution leads to both transverse and longitudinal energy imbalance, we do not force the W's to be exactly back-to-back. We introduce an extra momentum, $\vec{p}_{\text{extra}}$, Gaussian distributed in all three components and impose $\vec{p}_{\text{extra}} + \vec{W}_1 = -\vec{W}_2$, where $\vec{W}_{1,2}$ are the momenta of the two W's. For the longitudinal component the Gaussian has mean 0 and standard deviation 7.9 GeV, while for the transverse components the mean is randomly chosen as ± 0.5 GeV and the standard deviation is 1.4 GeV. These values were chosen to obtain reasonable agreement between the energy imbalance distributions of fully hadronic and mixed events.

In addition, we impose the following cuts which are related to the pre-selection of fully hadronic WW events [17]. We demand that the sphericity be larger than 0.045, that the total visible energy be larger than $0.7\sqrt{s}$, that the number of particles identified with the calorimeter (the cluster multiplicity) be larger than 30, that the ratio of the total longitudinal energy imbalance to the visible energy be smaller than 0.25, and that the y_{cut} value at which the event changes from a 3- to a 4-jet topology, y_{34}, be larger than 0.001. After forcing the event into 2 jets with the Durham clustering algorithm [22], the average of the jet masses is required to be larger than 30 GeV. After forcing the event into 4 jets with the Durham clustering algorithm, we assign two pairs of jets to each of the two W's by first rejecting the combination with the smallest dijet mass and then accepting the combination with the smallest difference between the two dijet masses (best pairing). We then demand that the difference between the two W masses be less than 70 GeV, that the smallest angle between any two jets be larger than 0.28 radians, and that the average of the two smallest angles between two jets from different W's be larger than 0.6 radians. These cuts reject only approximately 1% of the events and do not change the Q-distribution. The final selection of fully hadronic events uses a cut at 0.6 on the output of a neural network [17]. This cut is also applied to the mixed events, rejecting 7%.

We have checked the mixing procedure by comparing the distributions and quantities of a large number of variables between mixed events and fully hadronic WW events, including event shape variables, track and cluster multiplicities, and variables related to the W such as mass, energy and orientation. In general, good agreement is found. Typical examples are shown in Fig. 3.

Results

Fig. 4 shows the distributions of the three terms in the right-hand side of eq. (4) for the data. The distributions have not been corrected for detector effects, but MC-estimated background has been subtracted, using eq. (11), from ρ_2^{W} and ρ_2^{WW}. At low values of Q we observe more pairs of unlike-sign particles than pairs of like-sign particles, both in the two-particle densities for fully hadronic (Fig. 4a) and semi-hadronic (Fig. 4b) events. Furthermore, we observe that $\rho_{\mathrm{mix}}^{\mathrm{WW}}(\pm,\pm)$ and $\rho_{\mathrm{mix}}^{\mathrm{WW}}(+,-)$ coincide (Fig. 4c).

From these distributions, we compute $\Delta\rho$ for like-sign and unlike-sign particle pairs, eq. (4). The resulting raw data distributions are shown in Fig. 5. Also shown are the predictions of KORALW after full detector simulation, reconstruction and selection. Both the BEA and BES scenarios are shown.

The BEA scenario using BE_{32} shows an enhancement in the $\Delta\rho$ distribution for like-sign pairs (Fig. 5a), but also a small enhancement for unlike-sign pairs (Fig. 5b). The effect for unlike-sign pairs is larger if BE_0 is used. These implementations of BEC clearly affect both the like- and unlike-sign particle spectra. From Fig. 5a it is clear that only the BES scenario describes the $\Delta\rho(\pm,\pm)$ distribution, while the BEA scenario is disfavoured. In particular, considering Q-values up to 0.6 GeV, the confidence level (CL) for the BES and BEA scenarios are, respectively, 84% and 0.8%. The calculations of the confidence levels are based on statistical errors including bin-to-bin correlations.

In Fig. 6 we show the distributions of D and D' for like-sign and unlike-sign particle pairs, eqs. (5) and (6), for the raw data. For the double ratio D' we use the BES scenario of KORALW as the reference sample. Also shown in the figure are the predictions of KORALW for the scenarios BEA and BES. Again, it is clear that the BES scenario of KORALW describes the data, CL=87% for both $D(\pm,\pm)$ and $D'(\pm,\pm)$, while the BEA scenario is disfavoured, CL=0.5% for both $D(\pm,\pm)$ and $D'(\pm,\pm)$. When BE_0 is used instead of BE_{32}, the BEA scenario is even more strongly disfavoured: CL=0.08% for both $D(\pm,\pm)$ and $D'(\pm,\pm)$. Note that the D' distributions are by definition equal to unity (apart from statistical fluctuations) when KORALW without inter-W BEC is used. Note also that D is already close to unity for BES, so that the difference between D and D' is small, which supports the validity of the mixing procedure.

To estimate the strength of inter-W BEC, the $D'(\pm,\pm)$ distribution is fitted (from 0 to 1.4 GeV) by the following function

$$D'(Q) = (1 + \epsilon Q)\left(1 + \Lambda \exp(-k^2 Q^2)\right) \quad , \tag{13}$$

where ϵ, Λ and k are the fit parameters. The result of the fit ($\chi^2 = 16$ for 32 degrees of freedom) for the strength of inter-W BEC is

$$\Lambda = 0.001 \pm 0.026 \pm 0.015 \quad ,$$

where the first error is statistical and the second systematic. The statistical error and χ^2 have been scaled using $S_{\mathrm{bin-bin}} = 1.49$ to account for bin-to-bin correlations, in the same way as described in the previous section. This value of Λ is consistent with zero, *i.e.*, with no inter-W BEC. A similar fit was performed for the KORALW BEA distribution, resulting in $\Lambda = 0.127 \pm 0.007$ (statistical error only). The data disagree with this value by more than 4 standard deviations.

The systematic uncertainty on Λ is the sum in quadrature of the contributions listed in Table 3. The amount of background was varied by $\pm 10\%$. The choice of Monte Carlo was varied using PYTHIA and KORALW, both with no BEC at all as well as with only intra-W

BEC. Also the effect of various models of colour reconnection[†)] (CR) was included. A change in the fit range (± 0.4 GeV), a change in the bin size (from 40 to 80 MeV) and a change in the parametrization (removing the factor $(1+\epsilon Q)$ from the fit) also give contributions to the systematic uncertainty. Furthermore, the track and event selections were varied.

In the mixing procedure we allow a semi-hadronic WW event to be combined with all possible other semi-hadronic WW events. To be sure that this does not introduce a bias, the analysis was repeated for a mixed sample where every semi-hadronic event was used only once. The influence of the mixing procedure was also studied by not only combining oppositely charged W's, but also like-sign W's. The influence of the extra momentum $\vec{p}_{\mathrm{extra}}$, used in the event mixing, is also included as a systematic effect. The RMS of the systematic uncertainties due to these three changes in the mixing procedure is the systematic uncertainty listed in Table 3. The influence of the cut on the neural network output for the mixed events was investigated by removing the cut.

Furthermore, the effect of uncertainties in the energy calibration of the calorimeters was studied. Finally, we studied the influence of the $\mathrm{q\bar{q}}\tau\nu$ channel. Since this channel is the most difficult to identify, and therefore has relatively high background and low efficiency, we repeated the analysis without it.

To make the analysis possibly more sensitive to inter-W BEC, we repeated the analysis twice using different selections to increase the overlap of the W^+ and W^- decay products. Since BEC occur mainly among soft particles and the overlap is expected to be larger for these particles than for high-momentum ones, we first repeated the analysis using only tracks with momenta smaller than 1.5 GeV. Another way to increase the overlap is to require that jets from different W's be close together. We therefore repeated the analysis requiring that the average of the smallest two of the four angles between jets from different W's be less than 75°. This results in a reduction of approximately 60% in the number of fully hadronic WW events. Fig. 7 shows the distributions of $D'(\pm,\pm)$ for these two analyses. It is again clear that the BEA scenario is disfavoured, particularly for the low-momentum selection, while BES describes the data well. For the low-momentum sample we find CL=1.6% for BEA and CL=96% for BES, and for the sample with the angular cut we find CL= 10% for BEA and CL=93% for BES. Moreover, we find $\Lambda = 0.026 \pm 0.034$ for the low-momentum sample and $\Lambda = -0.019 \pm 0.029$ for the sample with the angular cut. Both values are consistent with zero. The errors here are statistical only, including bin-to-bin correlations.

Conclusion

Intra-W Bose-Einstein correlations have been found to be similar to those observed in Z decay to light quarks. An excess at small values of Q in the distributions of $\Delta\rho(\pm,\pm)$, $D(\pm,\pm)$ and $D'(\pm,\pm)$ is expected from inter-W BEC, but none is seen. These distributions agree well with KORALW using BE_{32} when inter-W BEC are not included, but not when they are. We thus find no evidence for BEC between identical pions originating from different W's and disfavour their implementation using the BE_{32} and BE_0 algorithms.

[†)]The so-called SKI, SKII, SKII′ [9] and GH [10] models, as implemented in PYTHIA, were used.

Acknowledgments

We wish to express our gratitude to the CERN accelerator divisions for the excellent performance of the LEP machine. We acknowledge the contributions of the engineers and technicians who have participated in the construction and maintenance of this experiment.

Author List

The L3 Collaboration:

M.Acciarri,[26] P.Achard,[19] O.Adriani,[16] M.Aguilar-Benitez,[25] J.Alcaraz,[25] G.Alemanni,[22] J.Allaby,[17] A.Aloisio,[28] M.G.Alviggi,[28] G.Ambrosi,[19] H.Anderhub,[48] V.P.Andreev,[6,36] T.Angelescu,[12] F.Anselmo,[9] A.Arefiev,[27] T.Azemoon,[3] T.Aziz,[10] P.Bagnaia,[35] A.Bajo,[25] L.Baksay,[43] A.Balandras,[4] S.V.Baldew,[2] S.Banerjee,[10] Sw.Banerjee,[10] A.Barczyk,[48,46] R.Barillère,[17] P.Bartalini,[22] M.Basile,[9] R.Battiston,[32] A.Bay,[22] F.Becattini,[16] U.Becker,[14] F.Behner,[48] L.Bellucci,[16] R.Berbeco,[3] J.Berdugo,[25] P.Berges,[14] B.Bertucci,[32] B.L.Betev,[48] S.Bhattacharya,[10] M.Biasini,[32] A.Biland,[48] J.J.Blaising,[4] S.C.Blyth,[33] G.J.Bobbink,[2] A.Böhm,[1] L.Boldizsar,[13] B.Borgia,[35] D.Bourilkov,[48] M.Bourquin,[19] S.Braccini,[19] J.G.Branson,[39] F.Brochu,[4] A.Buffini,[16] A.Buijs,[44] J.D.Burger,[14] W.J.Burger,[32] X.D.Cai,[14] M.Campanelli,[48] M.Capell,[14] G.Cara Romeo,[9] G.Carlino,[28] A.M.Cartacci,[16] J.Casaus,[25] G.Castellini,[16] F.Cavallari,[35] N.Cavallo,[37] C.Cecchi,[32] M.Cerrada,[25] F.Cesaroni,[23] M.Chamizo,[19] Y.H.Chang,[50] U.K.Chaturvedi,[18] M.Chemarin,[24] A.Chen,[50] G.Chen,[7] G.M.Chen,[7] H.F.Chen,[20] H.S.Chen,[7] G.Chiefari,[28] L.Cifarelli,[38] F.Cindolo,[9] C.Civinini,[16] I.Clare,[14] R.Clare,[14] G.Coignet,[4] N.Colino,[25] S.Costantini,[5] F.Cotorobai,[12] B.de la Cruz,[25] A.Csilling,[13] S.Cucciarelli,[32] T.S.Dai,[14] J.A.van Dalen,[30] R.D'Alessandro,[16] R.de Asmundis,[28] P.Déglon,[19] A.Degré,[4] K.Deiters,[46] D.della Volpe,[28] E.Delmeire,[19] P.Denes,[34] F.DeNotaristefani,[35] A.De Salvo,[48] M.Diemoz,[35] M.Dierckxsens,[2] D.van Dierendonck,[2] C.Dionisi,[35] M.Dittmar,[48] A.Dominguez,[39] A.Doria,[28] M.T.Dova,[18,♯] D.Duchesneau,[4] D.Dufournaud,[4] P.Duinker,[2] I.Duran,[40] H.El Mamouni,[24] A.Engler,[33] F.J.Eppling,[14] F.C.Erné,[2] P.Extermann,[19] M.Fabre,[46] M.A.Falagan,[25] S.Falciano,[35,17] A.Favara,[17] J.Fay,[24] O.Fedin,[36] M.Felcini,[48] T.Ferguson,[33] H.Fesefeldt,[1] E.Fiandrini,[32] J.H.Field,[19] F.Filthaut,[17] P.H.Fisher,[14] I.Fisk,[39] G.Forconi,[14] K.Freudenreich,[48] C.Furetta,[26] Yu.Galaktionov,[27,14] S.N.Ganguli,[10] P.Garcia-Abia,[5] M.Gataullin,[31] S.S.Gau,[11] S.Gentile,[35,17] N.Gheordanescu,[12] S.Giagu,[35] Z.F.Gong,[20] G.Grenier,[24] O.Grimm,[48] M.W.Gruenewald,[8] M.Guida,[38] R.van Gulik,[2] V.K.Gupta,[34] A.Gurtu,[10] L.J.Gutay,[45] D.Haas,[5] A.Hasan,[29] D.Hatzifotiadou,[9] T.Hebbeker,[8] A.Hervé,[17] P.Hidas,[13] J.Hirschfelder,[33] H.Hofer,[48] G. Holzner,[48] H.Hoorani,[33] S.R.Hou,[50] Y.Hu,[30] I.Iashvili,[47] B.N.Jin,[7] L.W.Jones,[3] P.de Jong,[2] I.Josa-Mutuberría,[25] R.A.Khan,[18] M.Kaur,[18,◇] M.N.Kienzle-Focacci,[19] D.Kim,[35] J.K.Kim,[42] J.Kirkby,[17] D.Kiss,[13] W.Kittel,[30] A.Klimentov,[14,27] A.C.König,[30] A.Kopp,[47] V.Koutsenko,[14,27] M.Kräber,[48] R.W.Kraemer,[33] W.Krenz,[1] A.Krüger,[47] A.Kunin,[14,27] P.Ladron de Guevara,[25] I.Laktineh,[24] G.Landi,[16] M.Lebeau,[17] A.Lebedev,[14] P.Lebrun,[24] P.Lecomte,[48] P.Lecoq,[17] P.Le Coultre,[48] H.J.Lee,[8] J.M.Le Goff,[17] R.Leiste,[47] P.Levtchenko,[36] C.Li,[20] S.Likhoded,[47] C.H.Lin,[50] W.T.Lin,[50] F.L.Linde,[2] L.Lista,[28] Z.A.Liu,[7] W.Lohmann,[47] E.Longo,[35] Y.S.Lu,[7] K.Lübelsmeyer,[1] C.Luci,[17,35] D.Luckey,[14] L.Lugnier,[24] L.Luminari,[35] W.Lustermann,[48] W.G.Ma,[20] M.Maity,[10] L.Malgeri,[17] A.Malinin,[17] C.Maña,[25] D.Mangeol,[30] J.Mans,[34] G.Marian,[15] J.P.Martin,[24] F.Marzano,[35] K.Mazumdar,[10] R.R.McNeil,[6] S.Mele,[17] L.Merola,[28] M.Meschini,[16] W.J.Metzger,[30] M.von der Mey,[1] A.Mihul,[12] H.Milcent,[17] G.Mirabelli,[35] J.Mnich,[17] G.B.Mohanty,[10] T.Moulik,[10] G.S.Muanza,[24] A.J.M.Muijs,[2] B.Musicar,[39] M.Musy,[35] M.Napolitano,[28] F.Nessi-Tedaldi,[48] H.Newman,[31] T.Niessen,[1] A.Nisati,[35] H.Nowak,[47] R.Ofierzynski,[48] G.Organtini,[35] A.Oulianov,[27] C.Palomares,[25] D.Pandoulas,[1] S.Paoletti,[35,17] P.Paolucci,[28] R.Paramatti,[35] H.K.Park,[33] I.H.Park,[42] G.Passaleva,[17] S.Patricelli,[28] T.Paul,[11] M.Pauluzzi,[32] C.Paus,[17] F.Pauss,[48] M.Pedace,[35] S.Pensotti,[26] D.Perret-Gallix,[4] B.Petersen,[30] D.Piccolo,[28] F.Pierella,[9] M.Pieri,[16] P.A.Piroué,[34] E.Pistolesi,[26] V.Plyaskin,[27] M.Pohl,[19] V.Pojidaev,[27,16] H.Postema,[14] J.Pothier,[17] D.O.Prokofiev,[45] D.Prokofiev,[36] J.Quartieri,[38] G.Rahal-Callot,[48,17] M.A.Rahaman,[10] P.Raics,[15] N.Raja,[10] R.Ramelli,[48] P.G.Rancoita,[26] A.Raspereza,[47] G.Raven,[39] P.Razis,[29] D.Ren,[48] M.Rescigno,[35] S.Reucroft,[11] S.Riemann,[47] K.Riles,[3] J.Rodin,[43] B.P.Roe,[3] L.Romero,[25] A.Rosca,[8] S.Rosier-Lees,[4] J.A.Rubio,[17] G.Ruggiero,[16] H.Rykaczewski,[48] S.Saremi,[6] S.Sarkar,[35] J.Salicio,[17] E.Sanchez,[17] M.P.Sanders,[30] M.E.Sarakinos,[21] C.Schäfer,[17] V.Schegelsky,[36] S.Schmidt-Kaerst,[1] D.Schmitz,[1] H.Schopper,[49] D.J.Schotanus,[30] G.Schwering,[1] C.Sciacca,[28] A.Seganti,[9] L.Servoli,[32] S.Shevchenko,[31] N.Shivarov,[41] V.Shoutko,[27] E.Shumilov,[27] A.Shvorob,[31] T.Siedenburg,[1] D.Son,[42] B.Smith,[33] P.Spillantini,[16] M.Steuer,[14] D.P.Stickland,[34] A.Stone,[6] B.Stoyanov,[41] A.Straessner,[1] K.Sudhakar,[10] G.Sultanov,[18] L.Z.Sun,[20] H.Suter,[48] J.D.Swain,[18] Z.Szillasi,[43,¶] T.Sztaricskai,[43,¶] X.W.Tang,[7] L.Tauscher,[5] L.Taylor,[11] B.Tellili,[24] C.Timmermans,[30] Samuel C.C.Ting,[14] S.M.Ting,[14] S.C.Tonwar,[10] J.Tóth,[13] C.Tully,[17] K.L.Tung,[7] Y.Uchida,[14] J.Ulbricht,[48] E.Valente,[35] G.Vesztergombi,[13] I.Vetlitsky,[27] D.Vicinanza,[38] G.Viertel,[48] S.Villa,[11] P.Violini,[17] M.Vivargent,[4] S.Vlachos,[5] I.Vodopianov,[36] H.Vogel,[33] H.Vogt,[47] I.Vorobiev,[27] A.A.Vorobyov,[36] A.Vorvolakos,[29] M.Wadhwa,[5] W.Wallraff,[1] M.Wang,[14] X.L.Wang,[20] Z.M.Wang,[20] A.Weber,[1] M.Weber,[1] P.Wienemann,[1] H.Wilkens,[30] S.X.Wu,[14] S.Wynhoff,[17] L.Xia,[31] Z.Z.Xu,[20] J.Yamamoto,[3] B.Z.Yang,[20] C.G.Yang,[7] H.J.Yang,[7] M.Yang,[7] J.B.Ye,[20] S.C.Yeh,[51] An.Zalite,[36] Yu.Zalite,[36] Z.P.Zhang,[20] G.Y.Zhu,[7] R.Y.Zhu,[31] A.Zichichi,[9,17,18] G.Zilizi,[43,¶] B.Zimmermann,[48] M.Zöller.[1]

1 I. Physikalisches Institut, RWTH, D-52056 Aachen, FRG[§]
III. Physikalisches Institut, RWTH, D-52056 Aachen, FRG[§]
2 National Institute for High Energy Physics, NIKHEF, and University of Amsterdam, NL-1009 DB Amsterdam, The Netherlands
3 University of Michigan, Ann Arbor, MI 48109, USA
4 Laboratoire d'Annecy-le-Vieux de Physique des Particules, LAPP,IN2P3-CNRS, BP 110, F-74941 Annecy-le-Vieux CEDEX, France
5 Institute of Physics, University of Basel, CH-4056 Basel, Switzerland
6 Louisiana State University, Baton Rouge, LA 70803, USA
7 Institute of High Energy Physics, IHEP, 100039 Beijing, China[△]
8 Humboldt University, D-10099 Berlin, FRG[§]
9 University of Bologna and INFN-Sezione di Bologna, I-40126 Bologna, Italy
10 Tata Institute of Fundamental Research, Bombay 400 005, India
11 Northeastern University, Boston, MA 02115, USA
12 Institute of Atomic Physics and University of Bucharest, R-76900 Bucharest, Romania
13 Central Research Institute for Physics of the Hungarian Academy of Sciences, H-1525 Budapest 114, Hungary[‡]
14 Massachusetts Institute of Technology, Cambridge, MA 02139, USA
15 KLTE-ATOMKI, H-4010 Debrecen, Hungary[¶]
16 INFN Sezione di Firenze and University of Florence, I-50125 Florence, Italy
17 European Laboratory for Particle Physics, CERN, CH-1211 Geneva 23, Switzerland
18 World Laboratory, FBLJA Project, CH-1211 Geneva 23, Switzerland
19 University of Geneva, CH-1211 Geneva 4, Switzerland
20 Chinese University of Science and Technology, USTC, Hefei, Anhui 230 029, China[△]
21 SEFT, Research Institute for High Energy Physics, P.O. Box 9, SF-00014 Helsinki, Finland
22 University of Lausanne, CH-1015 Lausanne, Switzerland
23 INFN-Sezione di Lecce and Universitá Degli Studi di Lecce, I-73100 Lecce, Italy
24 Institut de Physique Nucléaire de Lyon, IN2P3-CNRS,Université Claude Bernard, F-69622 Villeurbanne, France
25 Centro de Investigaciones Energéticas, Medioambientales y Tecnologícas, CIEMAT, E-28040 Madrid, Spain♭
26 INFN-Sezione di Milano, I-20133 Milan, Italy
27 Institute of Theoretical and Experimental Physics, ITEP, Moscow, Russia
28 INFN-Sezione di Napoli and University of Naples, I-80125 Naples, Italy
29 Department of Natural Sciences, University of Cyprus, Nicosia, Cyprus
30 University of Nijmegen and NIKHEF, NL-6525 ED Nijmegen, The Netherlands
31 California Institute of Technology, Pasadena, CA 91125, USA
32 INFN-Sezione di Perugia and Universitá Degli Studi di Perugia, I-06100 Perugia, Italy
33 Carnegie Mellon University, Pittsburgh, PA 15213, USA
34 Princeton University, Princeton, NJ 08544, USA
35 INFN-Sezione di Roma and University of Rome, "La Sapienza", I-00185 Rome, Italy
36 Nuclear Physics Institute, St. Petersburg, Russia
37 INFN-Sezione di Napoli and University of Potenza, I-85100 Potenza, Italy
38 University and INFN, Salerno, I-84100 Salerno, Italy
39 University of California, San Diego, CA 92093, USA
40 Dept. de Fisica de Particulas Elementales, Univ. de Santiago, E-15706 Santiago de Compostela, Spain
41 Bulgarian Academy of Sciences, Central Lab. of Mechatronics and Instrumentation, BU-1113 Sofia, Bulgaria
42 Laboratory of High Energy Physics, Kyungpook National University, 702-701 Taegu, Republic of Korea
43 University of Alabama, Tuscaloosa, AL 35486, USA
44 Utrecht University and NIKHEF, NL-3584 CB Utrecht, The Netherlands
45 Purdue University, West Lafayette, IN 47907, USA
46 Paul Scherrer Institut, PSI, CH-5232 Villigen, Switzerland
47 DESY, D-15738 Zeuthen, FRG
48 Eidgenössische Technische Hochschule, ETH Zürich, CH-8093 Zürich, Switzerland
49 University of Hamburg, D-22761 Hamburg, FRG
50 National Central University, Chung-Li, Taiwan, China
51 Department of Physics, National Tsing Hua University, Taiwan, China
§ Supported by the German Bundesministerium für Bildung, Wissenschaft, Forschung und Technologie
‡ Supported by the Hungarian OTKA fund under contract numbers T019181, F023259 and T024011.
¶ Also supported by the Hungarian OTKA fund under contract numbers T22238 and T026178.
♭ Supported also by the Comisión Interministerial de Ciencia y Tecnología.
♯ Also supported by CONICET and Universidad Nacional de La Plata, CC 67, 1900 La Plata, Argentina.
◇ Also supported by Panjab University, Chandigarh-160014, India.
△ Supported by the National Natural Science Foundation of China.

References

[1] G. Goldhaber *et al.*, Phys. Rev. Lett. **3** (1959) 181.

[2] D.H. Boal, C.K Gelbke, and B.K. Jennings, Rev. Mod. Phys. **62** (1990) 553; G. Baym, Acta Phys. Pol. **B 29** (1998) 1839.

[3] OPAL Collab., P.D. Acton *et al.*, Phys. Lett. **B 267** (1991) 143; ALEPH Collab., D. Decamp *et al.*, Z. Phys. **C 54** (1992) 75; DELPHI Collab., P. Abreu *et al.*, Phys. Lett. **B 286** (1992) 201; DELPHI Collab., P. Abreu *et al.*, Z. Phys. **C 63** (1994) 117; OPAL Collab., G. Alexander *et al.*, Z. Phys. **C 72** (1996) 389.

[4] L3 Collab., M. Acciarri *et al.*, Phys. Lett. **B 458** (1999) 517; DELPHI Collab., P Abreu *et al.*, Phys. Lett. **B 471** (1999) 460; OPAL Collab., G. Abbiendi *et al.*, *Transverse and Longitudinal Bose-Einstein Correlations in Hadronic Z^0 Decays*, Preprint CERN-EP-2000-004, CERN, 2000, submitted to E. Phys. J. **C**.

[5] L. Lönnblad and T. Sjöstrand, Phys. Lett. **B 351** (1995) 293; A. Ballestrero *et al.* in "Physics at LEP2", eds. G. Altarelli, T. Sjöstrand and P. Zwirner, CERN 96-01 (1996) 141; V. Kartvelishvili, R. Kvatadze and R. Møller, Phys. Lett. **B 408** (1997) 331; S. Jadach and K. Zalewski, Acta Phys. Pol. **B 28** (1997) 1363; K. Fiałkowski and R. Wit, Acta Phys. Pol. **B 28** (1997) 2039; K. Fiałkowski, R. Wit and J. Wosiek, Phys. Rev. **D 58** (1998) 094013.

[6] Š. Todorova-Nová, Ph.D. thesis, Strasbourg, IReS 98-18 (1998).

[7] L. Lönnblad and T. Sjöstrand, E. Phys. J. **C 2** (1998) 165.

[8] G. Gustafson, U. Pettersson and P. Zerwas, Phys. Lett. **B 209** (1988) 90; T. Sjöstrand and V.A. Khoze, Phys. Rev. Lett. **72** (1994) 28.

[9] T. Sjöstrand and V.A. Khoze, Z. Phys. **C 62** (1994) 281.

[10] G. Gustafson and J. Häkkinen, Z. Phys. **C 64** (1994) 659.

[11] L. Lönnblad, Z. Phys. **C 70** (1996) 107; C. Friberg, G. Gustafson and J. Häkkinen, Nucl. Phys. **B 490** (1997) 289; B.R. Webber, J. Phys. **G 24** (1998) 287.

[12] V.A. Khoze and T. Sjöstrand, E. Phys. J. **C 6** (1999) 271.

[13] DELPHI Collab., P. Abreu *et al.*, Phys. Lett. **B 401** (1997) 181; OPAL Collab., G. Abbiendi *et al.*, E. Phys. J. **C 8** (1999) 559; ALEPH Collab., R. Barate *et al.*, Phys. Lett. **B 478** (2000) 50; OPAL Collab., G. Abbiendi *et al.*, *Bose-Einstein Correlations in* $e^+e^- \to W^+W^-$ *Events at 172, 183 and 189 GeV,* OPAL Physics Note PN393, contrib. to HEP-EPS'99 conference, Tampere, Finland, 1999; ALEPH Collab., *Further studies on Bose-Einstein correlations in W-pair decay*, ALEPH-2000-039 CONF 2000-059, contrib. ICHEP 2000, Osaka, Japan, 2000; DELPHI Collab., P Abreu *et al.*, *Correlations between Particles in* $e^+e^- \to W^+W^-$ *Events*, DELPHI 2000-115 CONF 414, contrib. ICHEP 2000, Osaka, Japan, 2000.

[14] G. Goldhaber, S. Goldhaber, W. Lee and A. Pais, Phys. Rev. **120** (1960) 300.

[15] S.V. Chekanov, E.A. De Wolf, and W. Kittel, E. Phys. J. **C 6** (1999) 403.

[16] L3 Collab., B. Adeva *et al.*, Nucl. Inst. Meth. **A 289** (1990) 35; L3 Collab., O. Adriani *et al.*, Physics Reports **236** (1993) 1; M. Chemarin *et al.*, Nucl. Inst. Meth. **A 349** (1994) 345; M. Acciarri *et al.*, Nucl. Inst. Meth. **A 351** (1994) 300; I.C. Brock *et al.*, Nucl. Inst. Meth. **A 381** (1996) 236; A. Adam *et al.*, Nucl. Inst. Meth. **A 383** (1996) 342; G. Basti *et al.*, Nucl. Inst. Meth. **A 374** (1996) 293.

[17] L3 Collab., *Measurement of W-Pair Cross Sections and W-Decay Branching Fractions in* $\mathrm{e^+e^-}$ *Interactions at* $\sqrt{s} = 189$ *GeV*, Preprint CERN-EP-2000-104, CERN, 2000, submitted to Phys. Lett. **B**.

[18] KORALW version 1.33 is used; M. Skrzypek *et al.*, Comp. Phys. Comm. **94** (1996) 216; M. Skrzypek *et al.*, Phys. Lett. **B 372** (1996) 289.

[19] T. Sjöstrand, Comp. Phys. Comm. **82** (1994) 74.

[20] The L3 detector simulation is based on GEANT3, R. Brun *et al.*, CERN report CERN DD/EE/84-1 (Revised), 1987, and uses GHEISHA to simulate hadronic interactions, see H. Fesefeldt, RWTH Aachen report PITHA 85/02, 1985.

[21] L3 Collab., M. Acciarri *et al.*, Phys. Lett. **B 411** (1997) 373; A. Dominguez, Ph.D. thesis, University of California at San Diego (1998), http://hep.ucsd.edu/thesis/aaron.html.

[22] Yu. L. Dokshitzer, J. Phys. **G 17** (1991) 1537.

reference	MC, no BEC		(+, −) pairs	
channel	fully-hadronic	semi-hadronic	fully-hadronic	semi-hadronic
γ	$0.91 \pm 0.02 \pm 0.02$	$0.94 \pm 0.01 \pm 0.02$	$0.93 \pm 0.01 \pm 0.02$	$0.89 \pm 0.01 \pm 0.03$
λ	$0.55 \pm 0.04 \pm 0.07$	$0.70 \pm 0.06 \pm 0.05$	$0.48 \pm 0.05 \pm 0.07$	$0.64 \pm 0.07 \pm 0.05$
R (fm)	$0.56 \pm 0.04 \pm 0.06$	$0.64 \pm 0.05 \pm 0.06$	$0.71 \pm 0.04 \pm 0.05$	$0.75 \pm 0.05 \pm 0.06$
δ	$0.06 \pm 0.02 \pm 0.06$	$-0.01 \pm 0.01 \pm 0.06$	$0.07 \pm 0.01 \pm 0.05$	$0.07 \pm 0.02 \pm 0.05$
$S_{\text{bin-bin}}$	1.55 ± 0.09	1.30 ± 0.07	1.01 ± 0.08	1.07 ± 0.08
χ^2/ndf	13/31	24/31	28/31	31/31

Table 1: Values of the fit parameters γ, λ, R and δ, eq. (12), for the fully hadronic and the semi-hadronic WW events. Two different reference samples are used: KORALW without BEC, eq. (7), and unlike-sign particle pairs, eq. (8). The first error is statistical, the second systematic. The statistical error has been corrected by the factor $S_{\text{bin-bin}}$ to account for bin-to-bin correlations. The value of χ^2 has also been corrected for these correlations.

reference	MC, no BEC		(+, −) pairs	
channel	fully-hadronic	semi-hadronic	fully-hadronic	semi-hadronic
track selection	0.039	0.035	0.034	0.032
event selection	0.015	0.017	0.022	0.022
fit range	0.013	0.013	0.020	0.023
background fraction	0.011	0.008	0.009	0.007
other MC reference	0.014	0.015	0.019	0.018
other MC corr.	0.012	0.016	0.015	0.014
inter-W BE in MC corr.	0.051	–	0.048	–
Total	0.071	0.047	0.071	0.051

Table 2: Contributions to the systematic uncertainty of the λ parameter. Explanation of the sources is in the text.

source	contribution
background fraction	0.0021
other Monte Carlo (PYTHIA, BES or no BE)	0.0060
allowing CR in the reference sample	0.0024
fit range	0.0012
rebinning (40 $\rightarrow$ 80 MeV)	0.0024
removing $(1 + \epsilon Q)$ from the fit	0.0011
track selection	0.0073
event selection	0.0046
mixing	0.0040
neural net output cut	0.0039
energy calibration	0.0014
influence of τ channel	0.0076
total systematic uncertainty	0.015

Table 3: Contributions to the systematic uncertainty of the Λ parameter. Explanation of the sources is in the text.

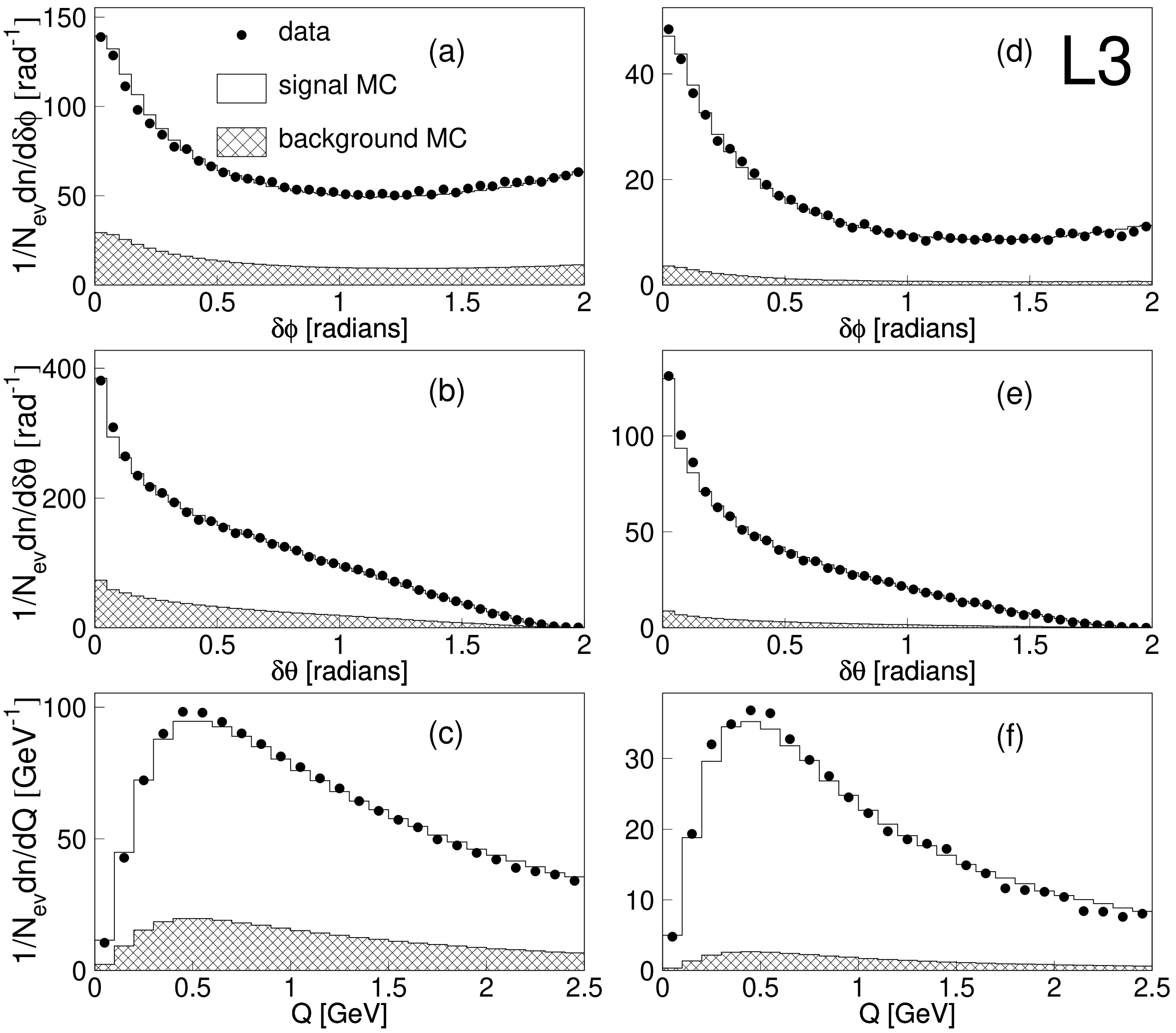

Figure 1: Distributions of (a, d) $\delta\phi$, the difference in azimuthal angle of pairs of tracks, (b, e) $\delta\theta$, the difference in polar angle of pairs of tracks, and (c, f) Q, the four-momentum difference, for the fully hadronic WW events (a–c) and for the semi-hadronic WW events (d–f). Only like-sign pairs of tracks are considered. The points are the uncorrected data, the open histograms are the expectation of KORALW with intra-W BEC plus background. The shaded histogram is the background expectation.

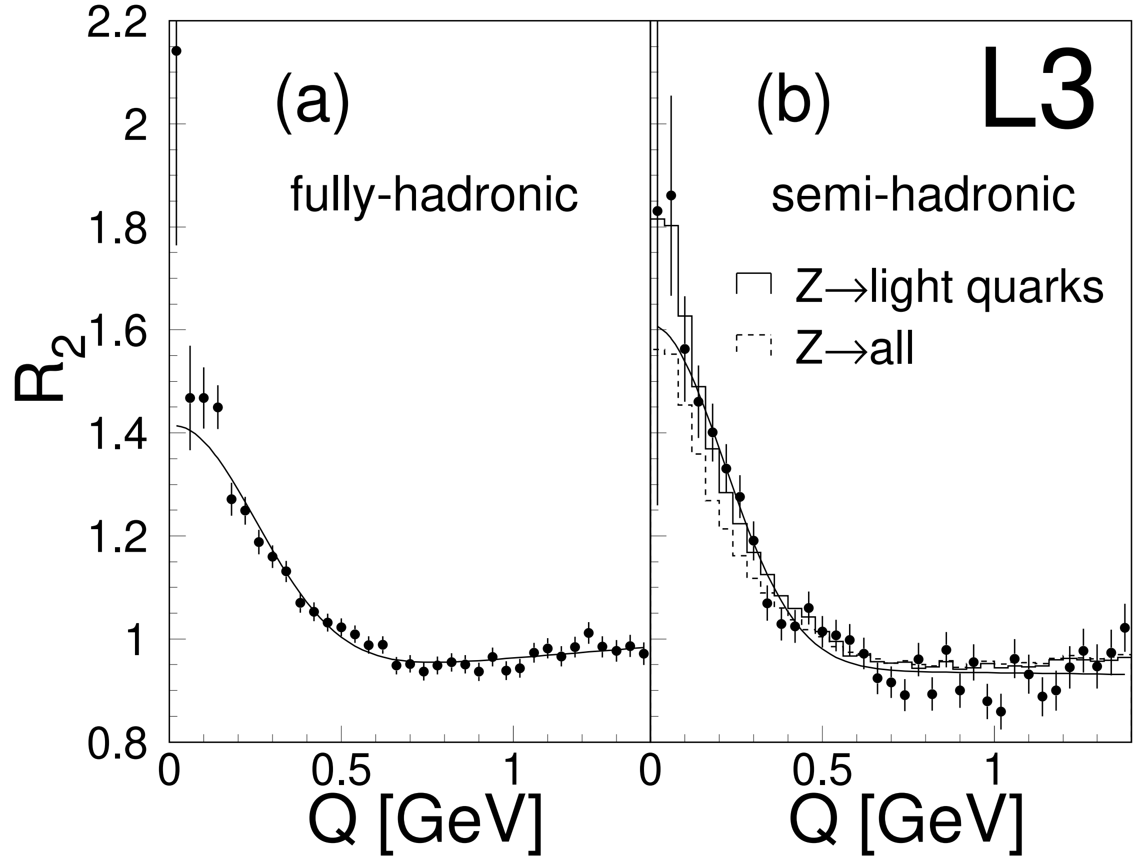

Figure 2: The Bose-Einstein correlation function R_2, eq. (9), for (a) the fully-hadronic WW events, and (b) the semi-hadronic WW events. In (b) the full histogram is for the light-quark Z decay sample and the dashed histogram is for a sample containing all hadronic Z decays. Also shown are the fits of eq. (12) to the WW data.

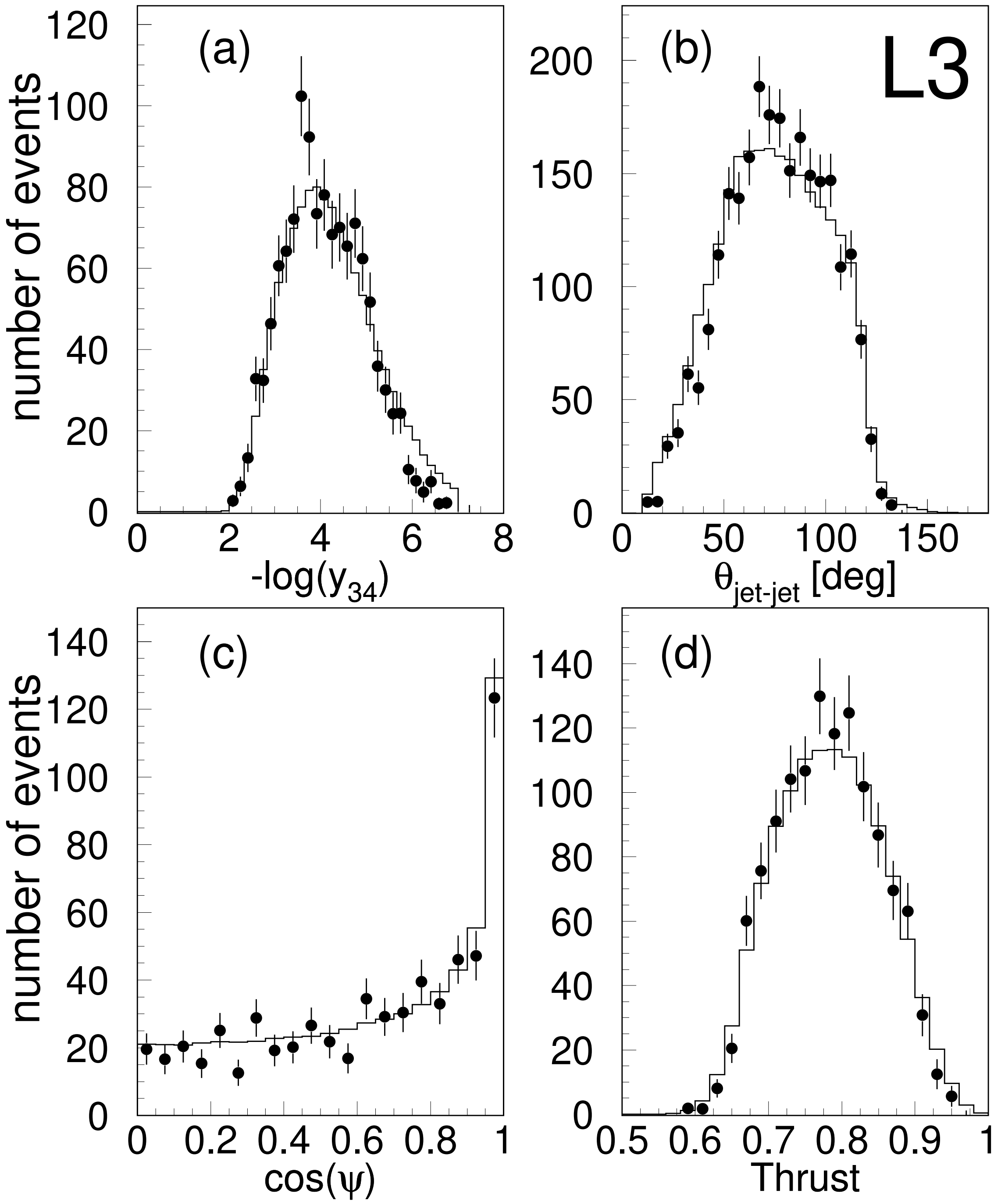

Figure 3: Comparison of uncorrected distributions for fully hadronic events after background subtraction (points) and mixed events (histograms): (a) $-\log y_{34}$; (b) the two smallest angles between jets of different W's, after jet finding and best pairing; (c) the cosine of the angle ψ between the decay planes of the two W's, after jet finding and best pairing; and (d) the event thrust.

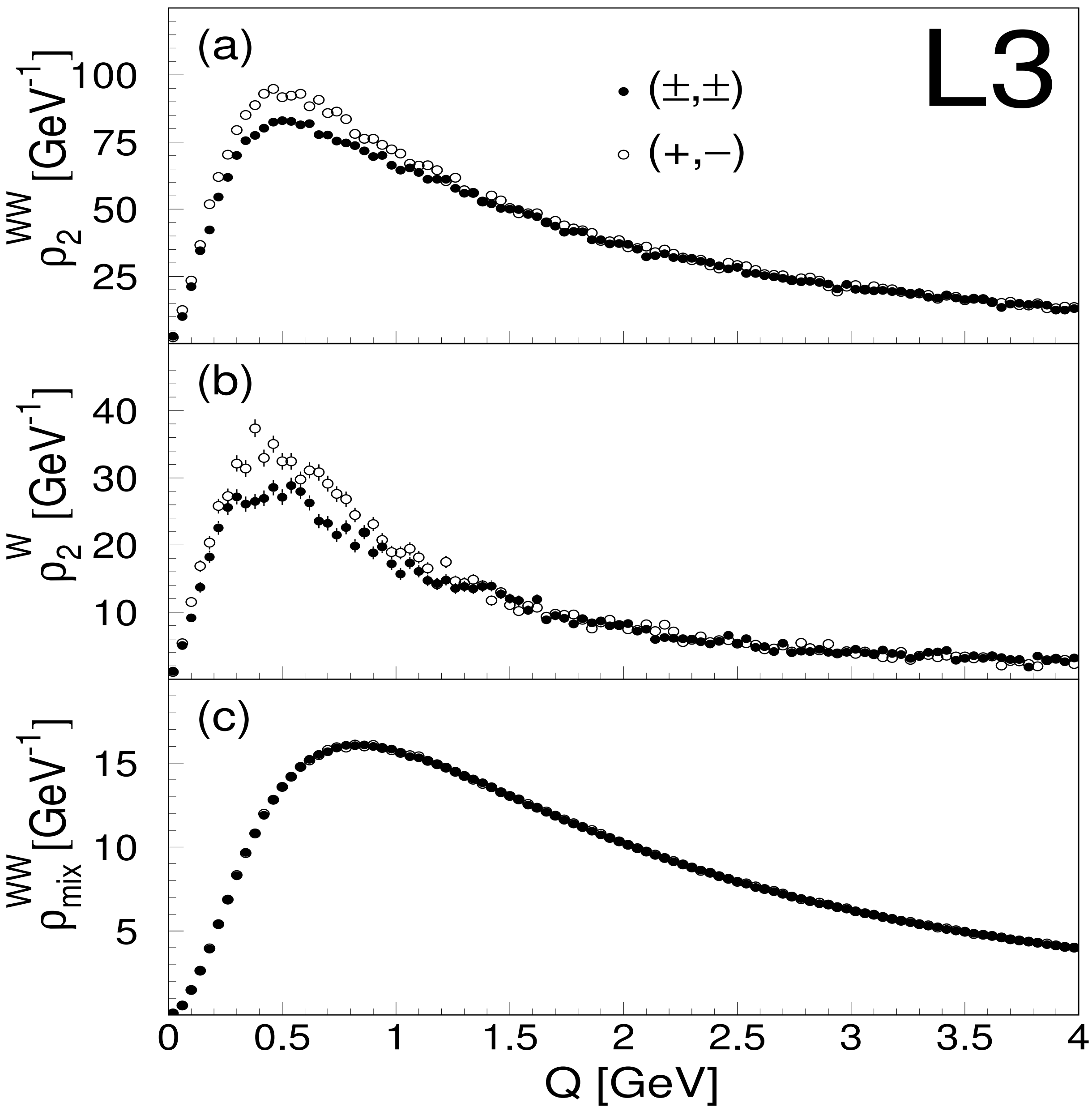

Figure 4: Distributions for uncorrected data of (a) $\rho_2^{\rm WW}$, (b) $\rho_2^{\rm W}$ and (c) $\rho_{\rm mix}^{\rm WW}$ for pairs of like-sign charged particles and pairs of unlike-sign charged particles.

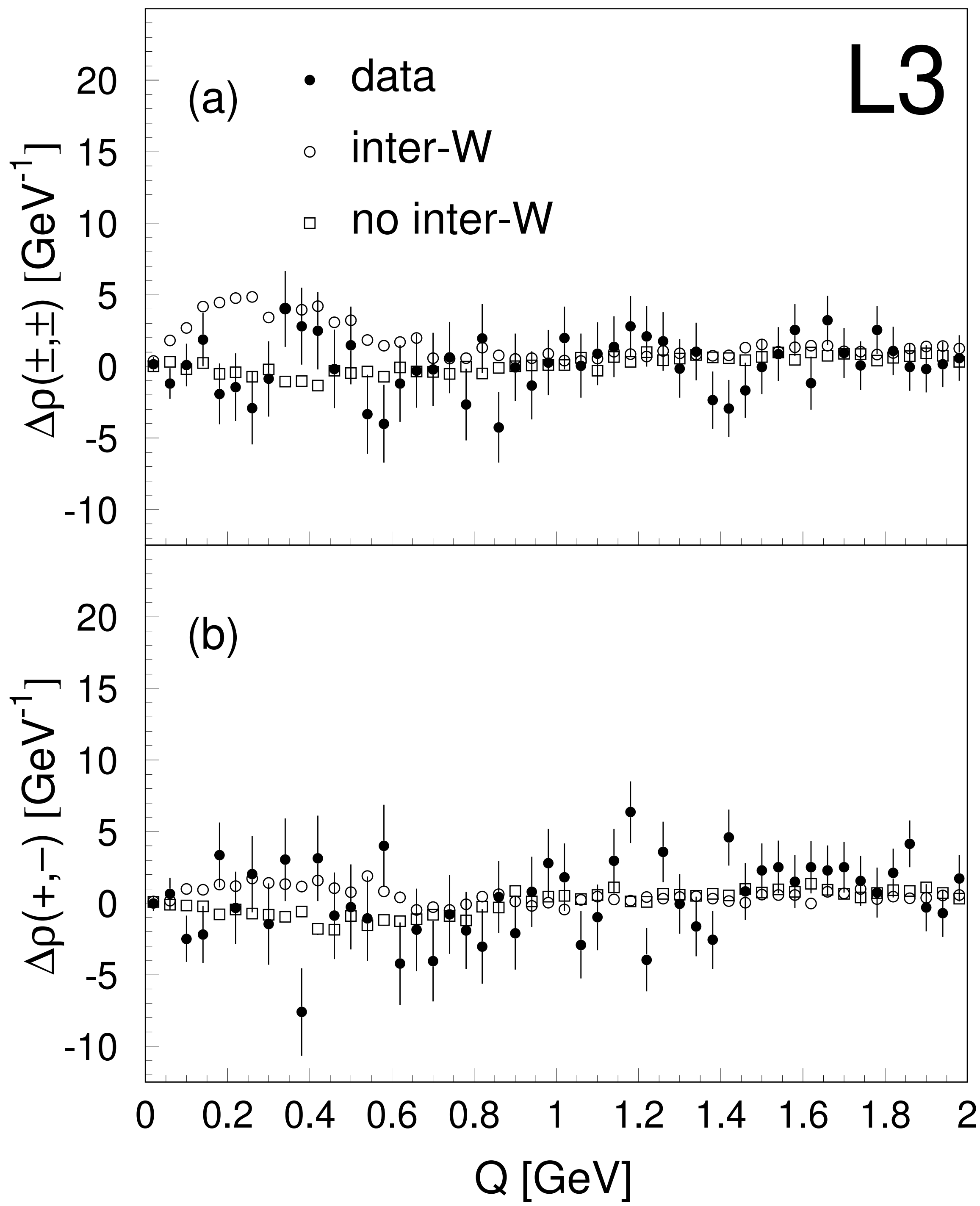

Figure 5: Distributions for uncorrected data of (a) $\Delta\rho(\pm,\pm)$ and (b) $\Delta\rho(+,-)$. Also shown are the Monte Carlo predictions of KORALW (at the detector level) with BEA (inter-W) and BES (no inter-W).

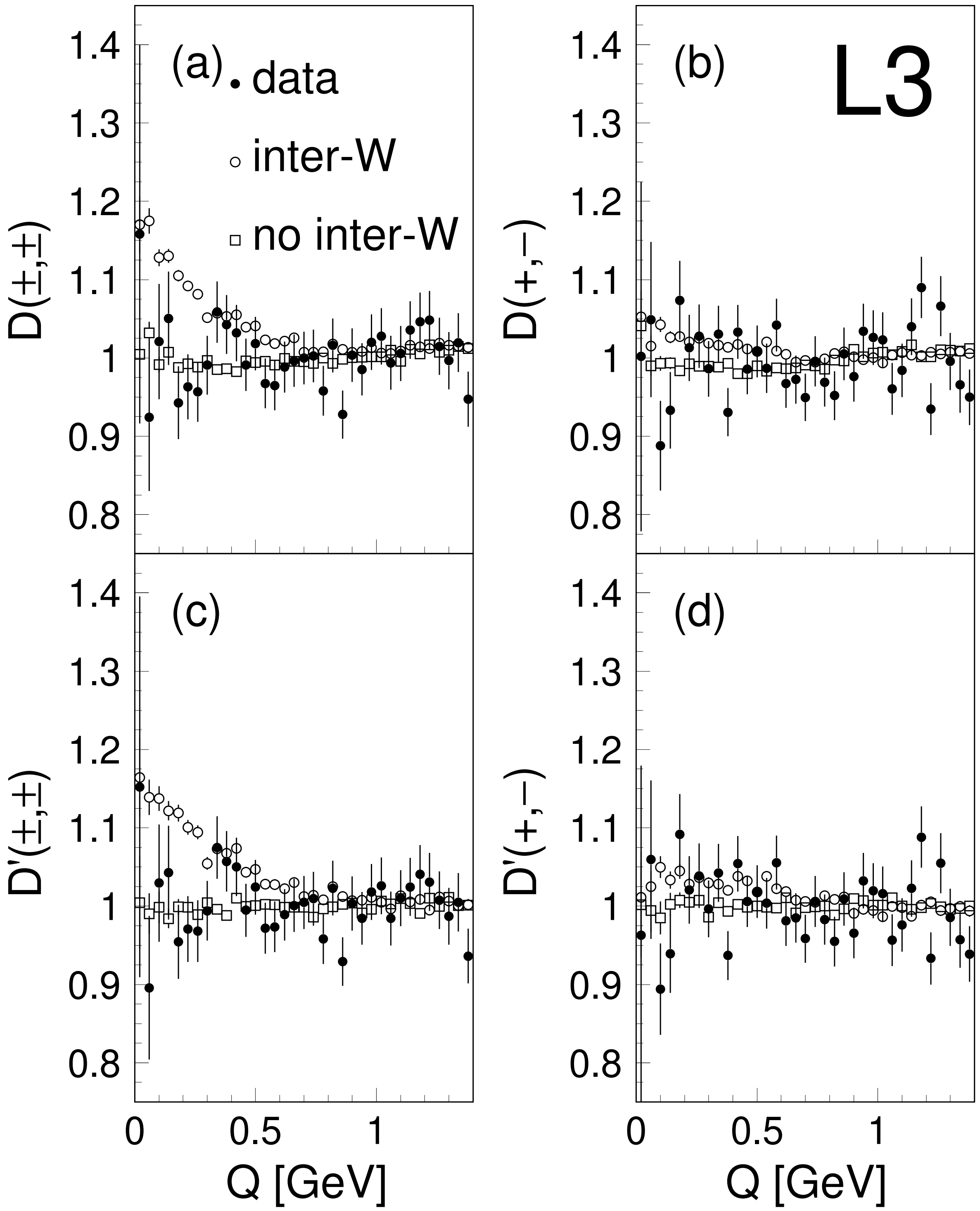

Figure 6: Distributions for uncorrected data of (a) $D(\pm,\pm)$, (b) $D(+,-)$, (c) $D'(\pm,\pm)$ and (d) $D'(+,-)$. Also shown are the predictions of KORALW (at the detector level) with BEA (inter-W) and BES (no inter-W).

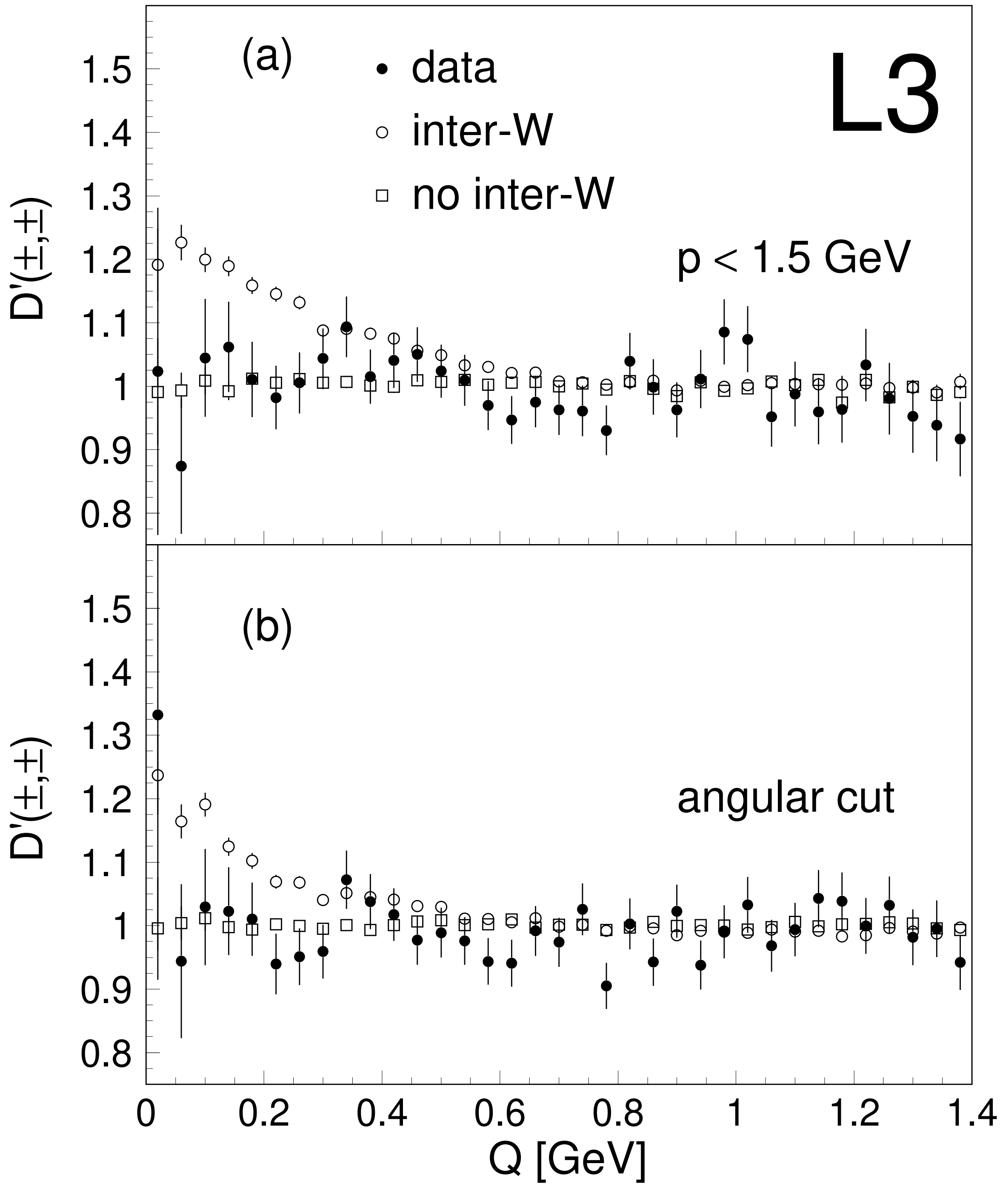

Figure 7: Distributions for uncorrected data of $D'(\pm,\pm)$ where (a) only low momentum tracks are used and (b) a cut is made on the average angle of the two smallest angles between jets of different W's. Also shown are the predictions of KORALW (at the detector level) with BEA (inter-W) and BES (no inter-W).